Recurrent *IDH2* Mutations in Salivary Gland Striated Duct Adenoma Define an Expanded Histologic Spectrum Distinct From Canalicular Adenoma

Lisa M. Rooper, MD,† Abbas Agaimy, MD,‡ Adel Assaad, MD,§ Munita Bal, MD,‖ Henrietta Eugene, BS,* Jeffrey Gagan, MD, PhD,¶ Hiro Nonogaki, MS,* Doreen N. Palsgrove, MD,¶ Akeesha Shah, MD,# Edward Stelow, MD,** Robert Stoehr, PhD,‡ Lester D.R. Thompson, MD,†† Ilan Weinreb, MD,‡‡§§ and Justin A. Bishop, MD¶*

Abstract: Striated duct adenoma (SDA) is a rare salivary gland neoplasm defined by histologic similarity to normal striated ducts. However, doubt persists about whether SDA represents a genuine entity distinct from canalicular adenoma and if a malignant counterpart exists. This study aims to evaluate the molecular underpinnings of SDA to clarify its pathogenesis and classification. We identified 10 SDA and 2 tumors called low-grade adenocarcinoma not otherwise specified that were retrospectively recognized to resemble SDA. All cases showed recurrent histologic features including (1) discrete monophasic tubules, (2) tall columnar eosinophilic cells, (3) monotonous oval nuclei, and (4) scant fibrous stroma, and most were positive for S100 protein (91%), SOX10 (80%), and CK7 (80%). Although 1 case was previously called adenocarcinoma based on interdigitation with normal acini, this pattern was also seen in some SDA, and likely does not indicate malignancy; the significance of growth surrounding nerve in 1 other case is less clear. Targeted sequencing identified *IDH2* R172X mutations in all 8 cases with sufficient tissue, with positivity for IDH1/2 mutation-specific immunohistochemistry in 9 cases stained. In contrast, 5 canalicular adenomas lacked *IDH2* mutations or other oncogenic alterations. Overall, *IDH2* R172X mutations are a defining feature of SDA that, in combination with its recognizable pathologic profile, confirm it is a unique entity separate from canalicular adenoma. IDH1/2 mutation-specific immunohistochemistry may provide a convenient tool to facilitate diagnosis. Both morphology and *IDH2* mutations raise parallels between SDA and breast tall cell carcinoma with reverse polarity.

Key Words: slivary gland neoplasms, striated duct adenoma, canalicular adenoma, adenocarcinoma not otherwise specified, *IDH2*, immunohistochemistry, molecular diagnostics

(*Am J Surg Pathol* 2023;47:333–343)

Striated duct adenoma (SDA) is a rare benign salivary gland tumor that is defined by its histologic similarity to normal striated ducts, including compact tubules composed of a monolayer of columnar epithelial cells with abundant eosinophilic cytoplasm. Although Dardick described the first ductal adenoma with striated duct features in 1996 and Weinreb et al characterized SDA in detail in 2010, only 10 cases of this entity have been described to date.[1–6] Indeed, there has been persistent doubt as to whether SDA is truly separate from canalicular adenoma, with the fourth edition World Health Organization (WHO) Classification of Head and Neck Tumors suggesting that the distinction between these 2 tumors is arbitrary.[7] Although SDA has formally been recognized as a unique salivary gland neoplasm in the fifth edition WHO Classification,[8] this tumor type remains poorly understood and infrequently recognized, and its genetic profile is entirely unknown. Furthermore, although at least 1 tumor has been reported as a low-grade salivary gland adenocarcinoma with striated duct differentiation,[9] it is unclear whether a true malignant counterpart of SDA exists and what criteria should define malignancy. In this study, we aim to evaluate the molecular underpinnings of salivary gland neoplasms with resemblance to striated ducts in hopes of better understanding their pathogenesis and classification.

From the *Department of Pathology; †Department of Oncology, The Johns Hopkins University School of Medicine, Baltimore, MD; ‡Institute of Pathology, Friedrich-Alexander-University Erlangen-Nürnberg, University Hospital, Erlangen, Germany; §Department of Pathology, Virginia Mason Hospital and Seattle Medical Center, Seattle, WA; ‖Department of Pathology, Tata Memorial Centre, Homi Bhabha National Institute, Mumbai, India; ¶Department of Pathology, University of Texas Southwestern Medical Center, Dallas, TX; #Department of Pathology, Cleveland Clinic Foundation, Cleveland, OH; **Department of Pathology, University of Virginia, Charlottesville, VA; ††Head and Neck Pathology Consultations, Woodland Hills, CA; ‡‡Department of Laboratory Medicine and Pathobiology, University of Toronto; and §§Department of Pathology, University Health Network, Toronto, ON.

A.A., I.W., and J.A.B. contributed equally.

This study was funded in part by the Jane B. and Edwin P. Jenevein, MD Endowment for Pathology at UT Southwestern Medical Center.

Conflicts of Interest and Source of Funding: The authors have disclosed that they have no significant relationships with, or financial interest in, any commercial companies pertaining to this article.

Correspondence: Justin A. Bishop, MD, University of Texas Southwestern Medical Center, 6201 Harry Hines Blvd, Dallas, TX, 75390-9073 (e-mail: Justin.Bishop@UTSouthwestern.edu).

MATERIALS AND METHODS

Case Selection

We identified 12 salivary gland striated duct neoplasms from the authors' surgical pathology archives and consultation files. Three of these tumors were reported in detail previously, including 2 that were included in the initial characterization of SDA[6] and 1 case report of SDA published subsequently.[2] There was also 1 case included in a large series of salivary adenocarcinoma not otherwise specified (NOS) that was retrospectively noted to have striated duct features.[9] For inclusion in this study, tumors had to display the morphologic features of SDA as defined in the fifth edition WHO Classification of Head and Neck Tumors, including tubules lined by a single layer of luminal cells that resemble normal striated ducts.[8] All available histologic sections were reviewed for each case, and the results of all existing immunohistochemical stains were tabulated. For comparison purposes, we also selected 5 cases of canalicular adenoma for analysis and documented their histologic features and existing immunohistochemical results.

Molecular Testing

We performed next-generation sequencing (NGS) on 5 striated duct neoplasms and 5 canalicular adenomas using a large targeted panel as described in detail previously.[10] In brief, DNA and RNA were isolated from formalin-fixed, paraffin-embedded tissue blocks using Qiagen AllPrep kits (Qiagen, Germantown, MD). An enriched library containing all exons from >1425 cancer-related genes was created using custom NimbleGen probes (Roche, Indianapolis, IN). Finally, sequencing was performed using a NextSeq. 550 (Illumina, San Diego, CA) with a median 900x target exon coverage. Variants were reviewed using the Integrated Genomics Viewer (Broad Institute, Cambridge, MA) and annotated using the gnomAD and dbSNP databases.

Based on NGS results, we also performed targeted sequencing of the *IDH1* and *IDH2* genes in 3 additional SDA. The hotspot regions of both genes (*IDH1* codon 132 and *IDH2* codon 172) were amplified after DNA isolation using the Qiagen multiplex PCR kit according to the manufacturer's instructions (Qiagen, Hilden, Germany) and the following primers: *IDH1*: forward: 5'- GCT TGT GAG TGG ATG GGT AAA -3', and reverse: 5'-Biotin TTG CCA ACA TGA CTT ACT TGA TC -3'; *IDH2*: 5' - TCC GGG AGC CCA TCA TCT – 3', and reverse: 5' – Biotin CCT GGC CTA CCT GGT CGC – 3'. Cycling conditions included: denaturation at 95°C for 2 min (1 cycle), 95°C for 30 sec, 53°C for 40 sec, 72°C for 40 sec (40 cycles), and a final 5 minutes extension at 72°C. Pyrosequencing was performed using the PyroMark Q24 (Qiagen) with single-stranded DNA prepared from 25 mL biotinylated PCR product with streptavidin-coated sepharose and 0.5 mM of the sequencing primer (IDH1: 5'- GGG TAA AAC CTA TCA TCA TA -3; IDH2: 5' - AGC CCA TCA CCA TTG - 3') using the PSQ Vacuum Prep Tool (Qiagen).

IDH2 Immunohistochemistry

Also, based on molecular results, we performed mutation-specific immunohistochemistry for IDH1/2 on 11 striated duct neoplasms. Seven of these cases had undergone molecular analysis and had additional tissue available. Whole-slide sections of these tumors were cut from formalin-fixed paraffin-embedded tissue blocks at 4 μm thickness. There were also 4 cases where no tissue block or unstained slides were available for molecular testing, and restaining was attempted on existing H&E slides. These slides were soaked in a 1:4 mix of acetone and xylene to remove the coverslip and were rehydrated sequentially in xylene (5 min × 3), 100% ethanol (1 min × 2), 95% ethanol (10 dips), 80% ethanol (10 dips), and water (10 dips). In addition, we performed IDH1/2 immunohistochemistry on previously-constructed tissue microarrays that contained 541 other salivary gland neoplasms.[9,11–14]

For all whole-slide sections, rehydrated H&E slides, and tissue microarray sections, staining was performed using a mouse monoclonal antibody recognizing mutant IDH1/2 protein (clone MsMab-1; 1:50 dilution; MilliporeSigma, Burlington, MA) resulting from *IDH1* R132 and *IDH2* R172 alterations. Antigen retrieval and staining were performed on Ventana BenchMark Ultra autostainers (Ventana Medical Systems, Tucson AZ) using standardized automated protocols in the presence of appropriate controls. Signals were visualized through the ultraView polymer detection kit (Ventana). Due to frequent nonspecific low-level blush in both tumor cells and normal structures, only granular cytoplasmic staining in >10% of tumor cells at a level above the background was regarded as positive.

RESULTS

Clinical Characteristics

Clinical and demographic information is summarized in Table 1. The striated duct neoplasms were taken from 6 men and 6 women with a median age of 59 years (range 23 to 81 y). The tumors most commonly affected the parotid gland (n = 10), but were also seen at minor salivary sites, including the palate (n = 1) and upper lip (n = 1). They had a median size of 1.5 cm (range 0.3 to 5 cm). While 10 cases were initially classified as SDA, 2 cases were originally signed out as low-grade adenocarcinoma, NOS. Because most cases were seen in consultation, detailed clinical and follow-up information was not available.

Histologic Features

All 12 striated duct neoplasms were composed of a monophasic population of eosinophilic cells predominantly arranged in compact, discrete tubules the size of normal striated ducts (Fig. 1A). These tubules ranged from crowded and back-to-back with attenuated lumens (Fig. 1B) to cystically dilated with thyroid-like eosinophilic serous secretions (Fig. 1C). The stroma was generally scant and fibrous, although several cases had areas with more stromal edema (Fig. 1D) or hemorrhage and 2 had a small amount of intermixed fat. The tumor

TABLE 1. Clinical, Molecular, and Immunohistochemical Features of Striated Duct Adenomas and Canalicular Adenomas

Case	Age	Sex	Site	Size (cm)	Original Diagnosis	Molecular (VAF)	IDH1/2 IHC
Striated duct adenomas							
1	45	F	Parotid	2.5	ACA NOS	*IDH2* R172G (33%)	Pos
2	62	M	Upper lip	0.9	SDA	ND	Failed
3	38	F	Parotid	2.5	SDA	*IDH2* R172S (26%)	Pos
4	81	M	Parotid	2	SDA	ND	Failed
5	47	F	Parotid	1.5	SDA	ND	Pos
6	57	F	Parotid	1.5	SDA	ND	Pos
7	23	M	Parotid	5	SDA	*IDH2* R172S (31%)	Pos
8	72	M	Parotid	0.8	ACA NOS	*IDH2* R172S (16%)	Pos
9	63	M	Parotid	1.2	SDA	*IDH2* R172G (24%)	Pos
10	77	F	Palate	0.3	SDA	*IDH2* R172T (18%)	Weak pos
11	60	F	Parotid	2	SDA	*IDH2* R172M (24%)	ND
12	41	M	Parotid	1.5	SDA	*IDH2* R172S (30%)	Pos
Canalicular adenomas							
1	73	M	Palate	1.9	CA	Neg	ND
2	90	F	Upper lip	1	CA	Neg	ND
3	84	F	Buccal	1.6	CA	Neg	ND
4	75	F	Upper lip	1	CA	Neg	ND
5	64	F	Upper lip	2	CA	Neg	ND

ACA NOS indicates adenocarcinoma not otherwise specified; CA, canalicular adenoma; ND, not done; Neg, negative; Pos, positive; SDA, striated duct adenoma; SMA, smooth muscle actin; SMM, smooth muscle myosin; VAF, variant allele fraction.

cells were tall columnar to cuboidal with crisp, well-defined cell membranes and homogenous eosinophilic cytoplasm (Fig. 2A). Occasional cytoplasmic vacuolation and granularity was seen (Fig. 2B). The nuclei had variable polarization, with many positioned in the middle or apex of the cell (Fig. 2C), and were largely oval with homogenous chromatin, single delicate nucleoli, and scattered intranuclear cytoplasmic inclusions (Fig. 2D). A few tumors displayed unusual features, including well-formed papillary fronds projecting into large cysts (Fig. 3A), slate-blue myxoid stroma (Fig. 3B), more complex anastomosing tubules with angulated and glomeruloid lumens (Fig. 3C), and overt oncocytic cytology with polygonal cells and abundant granular cytoplasm (Fig. 3D).

The 2 tumors originally classified as low-grade adenocarcinoma, NOS, had been previously designated as malignant on the basis of invasive growth. Both of these tumors included foci where neoplastic tubules interdigitated between adjacent normal acini just beyond the capsule of the tumor without desmoplastic stromal response (Fig. 4A); tumor surrounded a nerve in 1 case (Fig. 4B). However, these features were not unique to tumors designated as adenocarcinoma. While 7 of the SDA displayed smooth interfaces with surrounding salivary gland parenchyma with only minor peripheral multinodularity (Figs. 4C), 2 had areas of irregular growth between normal acini identical to what was seen in the tumors called adenocarcinoma (Fig. 4D), and 1 also closely abutted a nerve. No definite neurotropic extension of tumor nests within perineural spaces was seen. The tumors previously diagnosed as low-grade adenocarcinoma, NOS, were otherwise histologically similar to the rest of the SDA, with no nuclear pleomorphism, increased mitotic activity, or tumor necrosis.

Molecular Findings

The results of molecular testing are summarized in Table 1. Molecular analysis identified *IDH2* R172X mutations in all 8 cases tested, including R172S in 4 cases, R172G in 2 cases, R172T in 1 case, and R172M in 1 case. Although several variants of uncertain significance were also identified in the 5 cases tested using a large NGS panel, no other known oncogenic or clinically significant mutations or fusions were seen in any case, including both tumors originally designated as adenocarcinoma, NOS.

Immunohistochemical Features

The results of immunohistochemistry are also summarized in Table 1. Diffuse, strong nuclear and cytoplasmic S100 protein positivity was present in 10 of 11 striated duct neoplasms stained (91%, Fig. 5A), with concordant positivity for SOX10 in 4 of 5 tumors tested (80%). The single tumor with negativity for S100 protein and SOX10 had prominent oncocytic cytology. CK7 positivity was also present in 8 of 10 cases tested (80%). Although no cases evaluated showed diffuse positivity for p63, there were 4 cases (36%) that did demonstrate rare to patchy expression in a basal distribution (Fig. 5B). This finding was also most prominent in the case with oncocytic cells. All cases tested were negative for smooth muscle actin (n = 7), calponin (n = 5), smooth muscle myosin (n = 4), and DOG1 (n = 4).

The striated duct neoplasms that had tissue available for staining displayed strong IDH1/2 reactivity in a granular to globular cytoplasmic pattern in 8 cases (Fig. 5C) and weak patchy granular positivity in 1 case. This staining correlated with molecular evidence of *IDH2* mutations in 7 tumors that underwent sequencing, with strong staining in all 4 cases with *IDH2* R172S and 2 cases with *IDH2* R172G and weak staining in the single case

TABLE 1. *(Continued)*

CK7	S100 Protein	SOX10	p63	SMA	Calponin	SMM	DOG1
Striated duct adenomas							
Pos	Pos	Pos	Neg	Neg	Neg	Neg	ND
ND	Pos	ND	Neg	ND	ND	ND	ND
Pos	Pos	ND	Neg	Neg	Neg	ND	ND
ND	ND	ND	ND	ND	ND	ND	ND
Pos	Pos	ND	Rare basal	Neg	Neg	Neg	ND
Pos	Pos	ND	Rare basal	Neg	Neg	Neg	ND
Pos	Pos	ND	Rare basal	Neg	ND	ND	ND
Pos	Neg	Neg	Patchy basal	ND	Neg	Neg	Neg
Pos	Pos	Pos	Neg	Neg	ND	ND	Neg
Neg	Pos	Pos	Neg	Neg	ND	ND	Neg
Pos	Pos	Pos	Neg	ND	ND	ND	Neg
Neg	Pos	ND	Neg	ND	ND	ND	ND
Canalicular adenomas							
Pos	Pos	ND	Focal	Neg	Neg	Neg	ND
Pos	Pos	ND	Neg	Neg	Neg	Neg	ND
Pos	Pos	ND	Focal	Neg	Neg	Neg	ND
Pos	Pos	ND	Focal	Neg	Neg	Neg	ND
Pos	Pos	ND	Focal	Neg	Neg	Neg	ND

with *IDH2* R172T. There were 2 cases that did not have sufficient tissue for molecular testing but also showed strong IDH1/2 immunohistochemical positivity in restained H&E sections. Although most cases displayed diffuse reactivity in 70% to 90% of tumor cells, the 1 case with weaker staining had patchy positivity in 20% of cells. In addition, interpretation in 1 case was complicated by fixation artifact, but strong staining was seen in well-preserved areas that comprised >10% of the tumor and was interpreted as positive. There were also 2 restained cases that were not interpretable due to a lack of any reactivity. Notably, IDH1/2 immunohistochemistry frequently showed a weak nonspecific blush in the eosinophilic granular cytoplasm of normal striated ducts (Fig. 5D), and staining was only considered positive if it was stronger than this background.

Canalicular Adenomas

Clinical, immunohistochemical, and molecular findings in the canalicular adenomas are also noted in Table 1. The 5 canalicular adenomas arose in 4 women and 1 man with a median age of 75 years (range 64 to 90 y). All tumors were located in minor salivary glands, including the upper lip (n = 3), palate (n = 1), and buccal mucosa (n = 1), and had a median size of 1.6 cm (range 1 to 1.9 cm). They showed classic histologic features for this entity, including beaded ribbons and cords and interconnecting tubules composed of columnar cells with eosinophilic cytoplasm that were embedded in an abundant myxoid stroma. Immunohistochemically, all 5 cases (100%) were positive for CK7 and S100 protein, 4 (80%) had patchy p63 reactivity, and all 5 (0%) were negative for SMA, calponin, and smooth muscle myosin. By NGS, all 5 canalicular adenomas were negative for *IDH2* alterations and lacked other oncogenic or clinically significant mutations or fusions.

IDH1/2 Immunohistochemistry

The results of IDH1/2 mutation-specific immunohistochemistry performed on 541 salivary gland neoplasms included on TMAs are noted in Table 2. Among this cohort, there were 23 other salivary tumors (4%) that showed >10% moderate to strong staining for IDH1/2. However, in almost all of those cases, staining was not diffuse and was present in less than 50% of tumor cells. Only 4 cases, including 2 salivary duct carcinomas and 2 mucoepidermoid carcinomas, showed diffuse, strong IDH1/2 immunohistochemical expression in 70% to 90% of tumor cells—similar to the level seen in SDA. Both salivary duct carcinomas had previously undergone targeted next-generation sequencing utilizing commercially-available panels and did not have evidence of *IDH2* or *IDH1* mutations. The mucoepidermoid carcinomas also had previously shown *MAML2* gene rearrangement using fluorescence in-situ hybridization.[11]

DISCUSSION

SDA are rare salivary gland tumors that remain infrequently diagnosed and poorly understood despite recent codification in the fifth edition WHO Classification of Head and Neck Tumors.[8] In the largest series of these tumors to date, we confirm previous reports of their distinctive and recognizable histologic profile, including (1) discrete, compact tubules with variable cystic change, (2) a monophasic population of tall columnar to cuboidal cells with homogenous eosinophilic cytoplasm, (3) monotonous oval nuclei with occasional nuclear inclusions and variable polarization, and (4) scant fibrous to edematous stroma with occasional hemorrhage and fat. Notably, we also

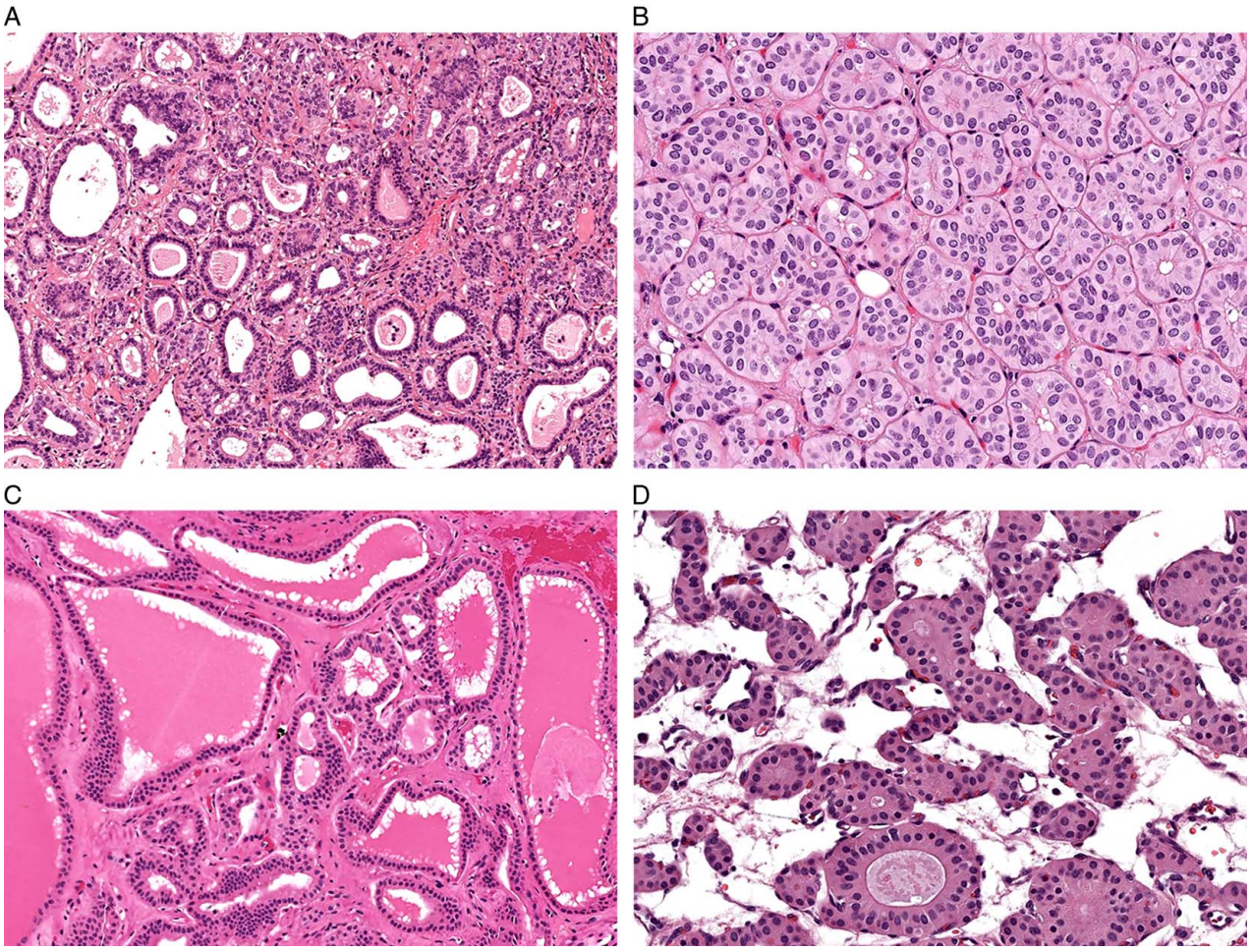

FIGURE 1. SDA was composed of a monophasic population of eosinophilic cells arranged in compact tubules similar in size to normal striated ducts (A, ×10). While some tubules had attenuated lumens and were crowded back-to-back (B, ×20), others were cystically dilated and contained eosinophilic serous secretions that mimicked thyroid follicles (C, ×10), and some had a moderate amount of edematous to fibrous stroma (D, ×20).

highlight unusual histologic features in a few cases that expand the spectrum of SDA, including large cysts with well-formed papillary fronds, slate-blue myxoid stroma, complex anastomosing tubules, and well-developed oncocytic change. Most cases do demonstrate immunohistochemical positivity for CK7 and S100 protein, as previously reported, and we also document unsurprising SOX10 expression. However, these stains are not perfectly sensitive for SDA and can be negative in cases with diagnostic histologic and molecular features. Occasional p63 positivity in a basal distribution is also present in a significant subset of cases despite the absence of a clear biphasic cell population and negativity for other myoepithelial markers; this finding was particularly prominent in a case with oncocytic differentiation and parallels staining seen in other oncocytic salivary gland tumors.[15] Awareness of these histologic and immunohistochemical features should allow pathologists to more consistently recognize SDA.

These results also raise questions as to whether a true malignant counterpart to SDA exists, despite sometimes irregular borders. One tumor in this series was originally called adenocarcinoma, NOS, on the sole basis of interdigitation between normal acini, with striated duct features only appreciated retrospectively. However, previously reported cases of SDA have demonstrated an irregular interface with surrounding salivary gland tissue, possibly representing associated striated duct hyperplasia[6]—a finding also seen in 2 additional adenomas in this series. Indeed, this growth pattern is reminiscent of the transition between basal cell adenomas and their precursor intercalated duct lesions, which interdigitate with normal parotid tissue.[16] As such, a small amount of peripheral irregularity just beyond the tumor capsule should not be regarded as indicative of malignancy in these tumors. The presence of tumor surrounding a nerve in 1 case initially called adenocarcinoma NOS is far more worrisome, although 1 tumor diagnosed as SDA also closely abutted

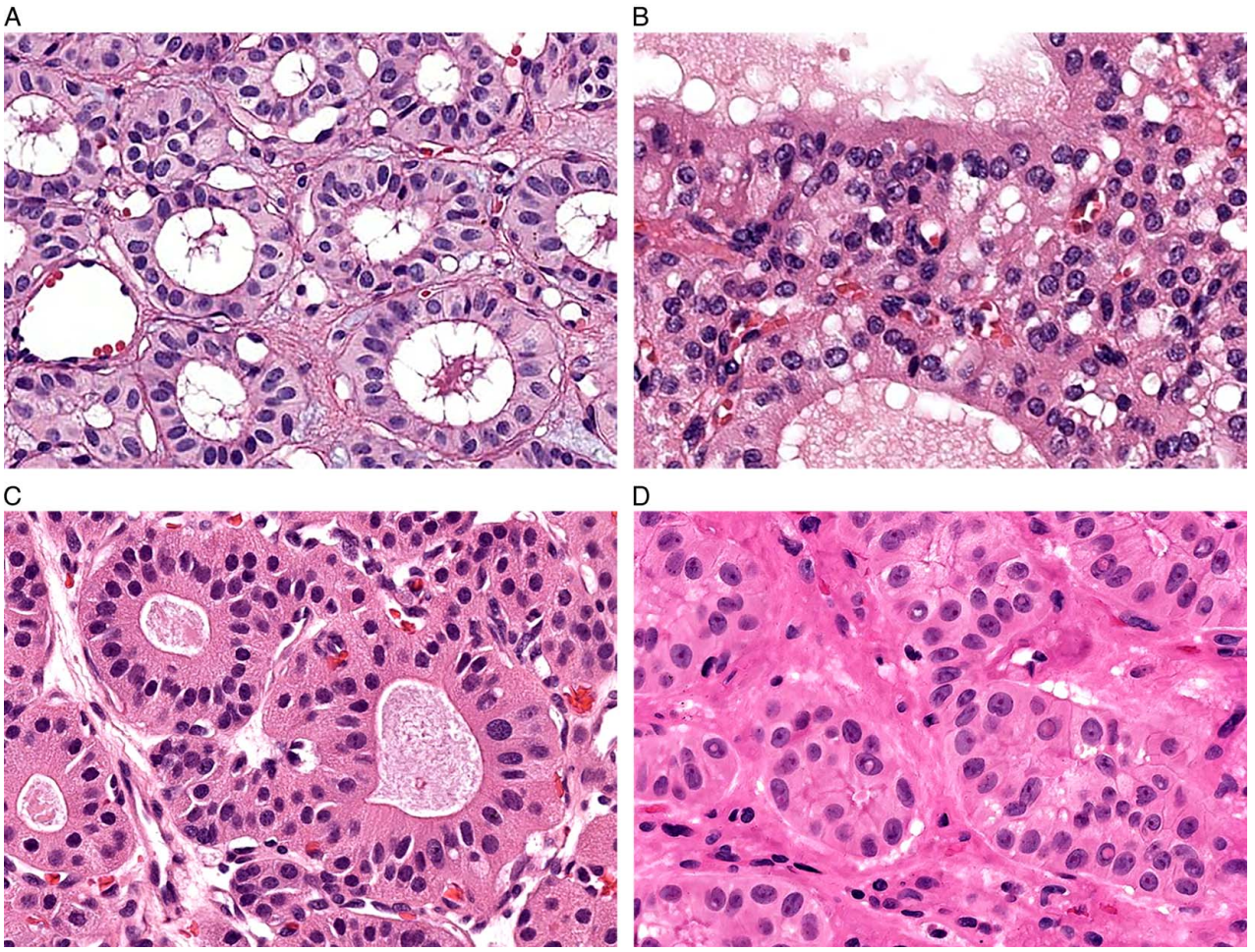

FIGURE 2. SDA displayed tall columnar to cuboidal cells with well-defined cell borders and homogenous eosinophilic cytoplasm (A, ×20) that showed occasional vacuolation (B, ×20). The nuclei had variable polarization, including localization to the middle and apex of the cells in a subset of cases (C, ×20), and were uniform and oval with homogenous chromatin, single delicate nucleoli, and scattered intranuclear cytoplasmic inclusions (D, ×20).

nerve. No definite violation of the perineurium was seen in either case, suggesting that this finding may represent secondary entrapment of nerves rather than true neurotropic spread. Moreover, there is precedent for other benign salivary processes to surround nerves, as multinodular oncocytic hyperplasia and intercalated duct hyperplasia are thought to gradually replace salivary lobules and entrap serous acini, normal ducts, and even nerves. Nevertheless, in the absence of long-term clinical follow-up, it is difficult to determine the significance of growth adjacent to nerves in striated duct neoplasms. Ultimately, while more experience is needed to rule out the existence of a genuine striated duct adenocarcinoma in tumors that abut nerves, recognition of striated duct features should discourage diagnosis of carcinoma based on irregular borders alone.

These results also demonstrate the unifying presence of recurrent *IDH2* mutations in SDA. All SDA in this series that underwent successful analysis showed *IDH2* R172X mutations by either molecular testing or immunohistochemistry. The *IDH2* gene on chromosome 15q26.1 encodes a mitochondrial enzyme that catalyzes the oxidative decarboxylation of isocitrate as part of the tricarboxylic acid cycle (Krebs cycle). *IDH2* hotspot mutations affect the conformation of the enzyme active site, leading to the production of an oncometabolite that increases cellular proliferation and impairs differentiation.[17–19] Although its paralog *IDH1* is more common in tumors in general, recurrent *IDH2* mutations have been identified in gliomas, acute myeloid leukemia, chondrosarcoma, and cholangiocarcinoma.[20–23] In the head and neck, *IDH2* mutations were recently recognized as the principal driver of high-grade carcinomas classified as sinonasal undifferentiated carcinoma and large cell neuroendocrine carcinoma.[24,25] Our findings demonstrate that salivary SDA is another tumor type with recurrent *IDH2* mutations. *IDH2* mutations have never previously been identified as either a defining molecular feature or even a rare event in large molecular profiling studies of most common salivary gland malignancies.[26–41] As such, this finding represents the first role for *IDH2* in salivary gland tumors.

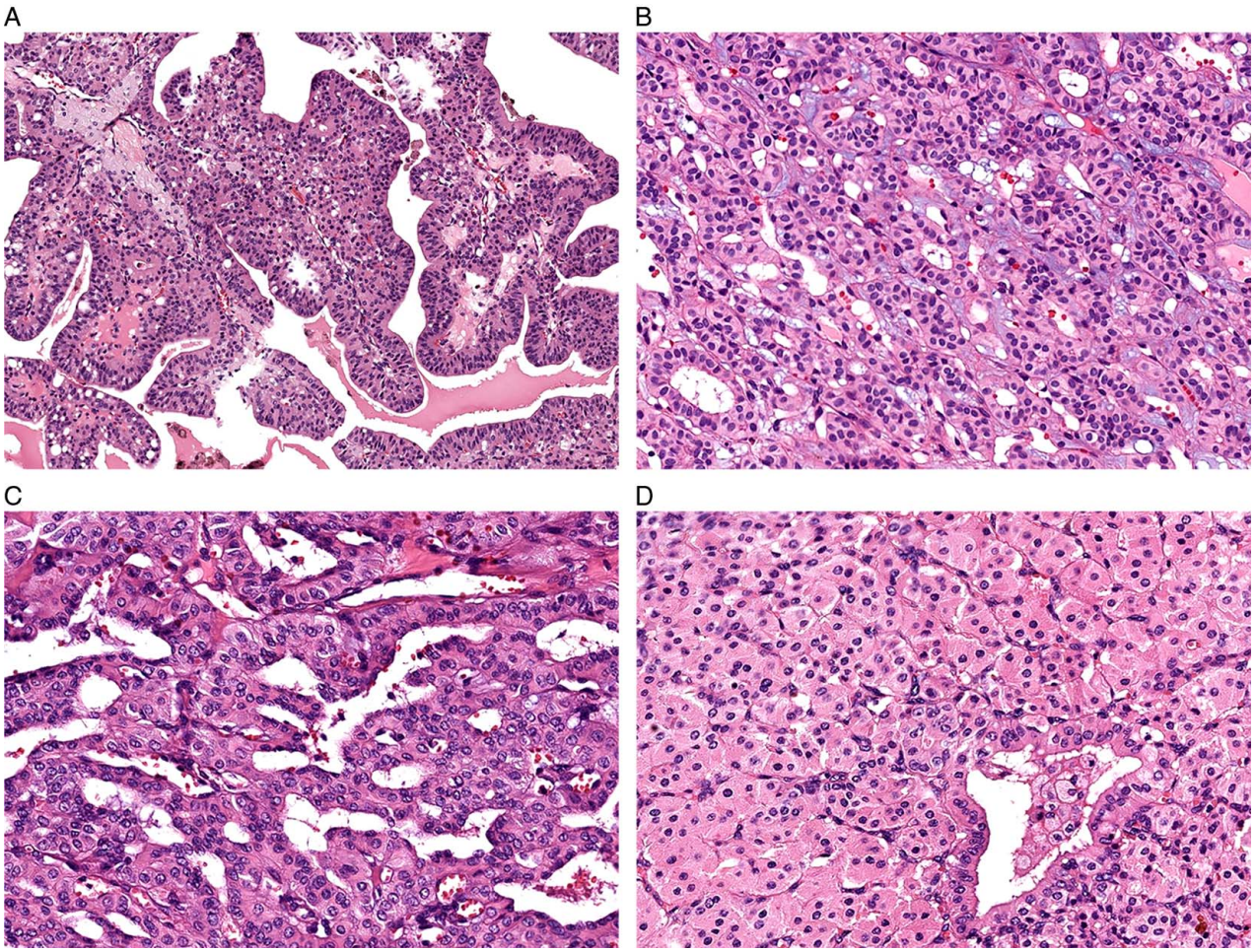

FIGURE 3. A few SDA had unique histologic features including larger cystic spaces with well-formed papillary fronds (A, ×4), slate-blue myxoid stroma (B, ×10), more complex architecture with anastomosing tubules and irregular luminal contours (C, ×20), and well-developed oncocytic change including granular cytoplasm and round nuclei with prominent nucleoli (D, ×20).

Importantly, recurrent *IDH2* mutations underscore SDA's existence as a distinctive salivary gland entity and differentiate it from overlapping salivary gland neoplasms, particularly canalicular adenoma. As recently as the fourth edition WHO Classification of Head and Neck Tumors, the distinction between SDA and canalicular adenomas was described as arbitrary.[7] Indeed, these tumors have striking histologic and immunohistochemical parallels, including monophasic populations of columnar eosinophilic cells and consistent S100 protein reactivity.[42] However, key morphologic differences have long indicated they are separate entities, with SDA demonstrating discrete, crowded tubules, minimal stroma, and abundant cytoplasm and canalicular adenoma displaying variable and complex architecture, abundant stroma, and hyperchromatic and elongated nuclei.[6] Now, identification of *IDH2* mutations in SDA but not canalicular adenoma cements the clear distinction between these tumor types. Notably, the molecular profile of canalicular adenoma remains enigmatic, with no recurrent mutations or fusions in this or previous studies.[43] This absence of recognizable alterations likely reflects the involvement of obscure genes not currently included on sequencing panels or epigenetic changes. While other overlapping salivary tumors, including pleomorphic adenoma, myoepithelioma, basal cell adenoma, oncocytoma, and intercalated duct adenoma, can be more easily distinguished from SDA histologically, *IDH2* mutations provide an additional point of separation from these entities as well.

Conversely, both the morphology and *IDH2* mutations set up striking parallels between SDA and tall cell carcinoma with reversed polarity (TCCRP) of the breast. Previously reported as a breast tumor resembling a tall cell variant of papillary thyroid carcinoma and solid papillary carcinoma with reverse polarity, TCCRP is a rare breast tumor defined by columnar cells with

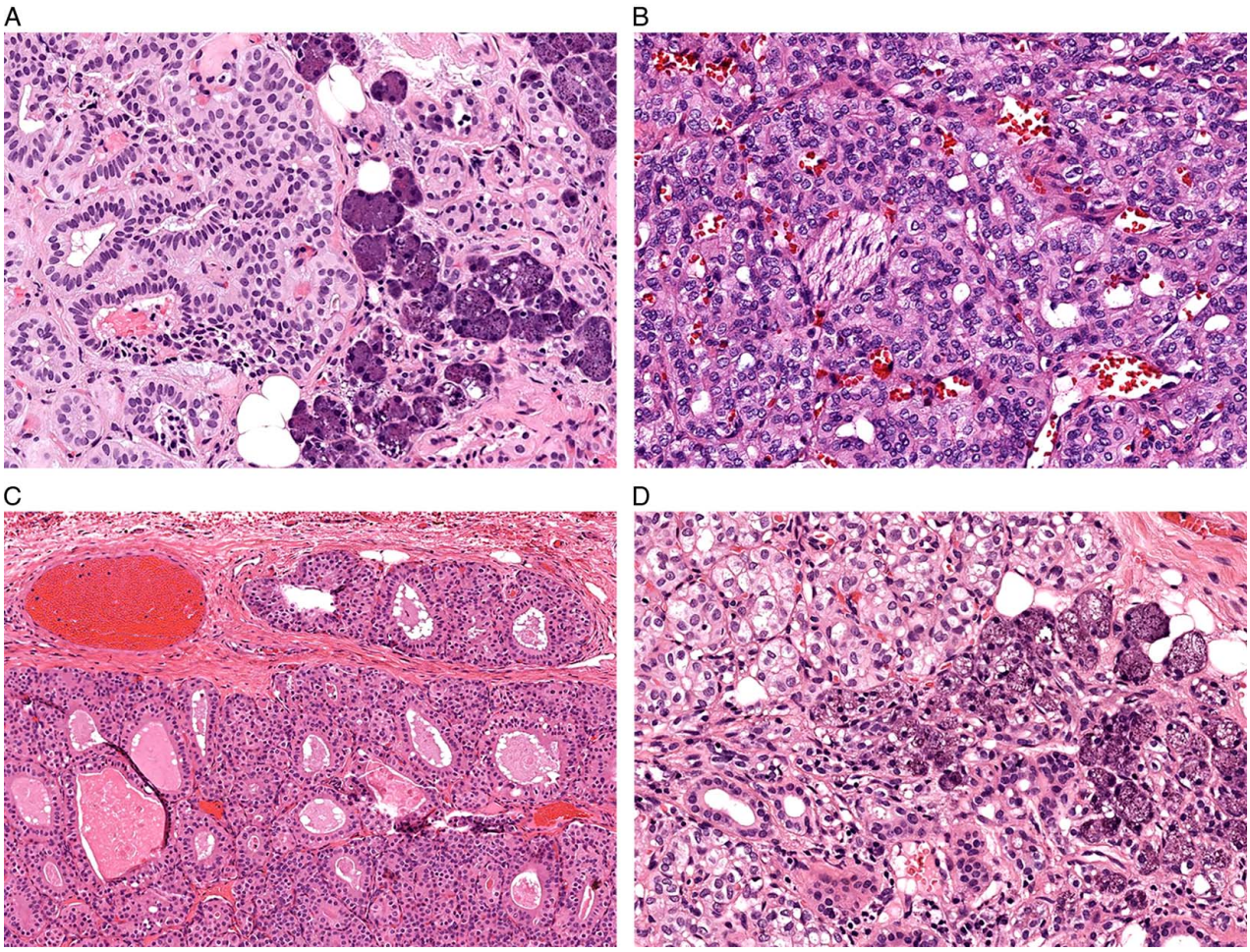

FIGURE 4. Tumors originally classified as low-grade adenocarcinoma, NOS showed areas where tumor follicles interdigitated between normal acini (A, ×10) or surrounded nerve (B, ×20). While most cases classified as SDA showed a smooth interface with surrounding tissue with only occasional peripheral multinodularity (C, ×10), a few also interdigitated between normal parenchyma (D, ×20), casting doubt on irregular borders as a specific indicator of malignancy.

eosinophilic cytoplasm and nuclei that polarize toward the apical aspect of the cell.[44] TCCRP are not entirely identical to salivary striated duct neoplasms at the histologic level, as the breast tumors show more irregular borders, complex papillary architecture, and diffuse reverse nuclear polarization. Nevertheless, the tall columnar cells, abundant eosinophilic cytoplasm, and uniform oval nuclei seen in TCCRP are strikingly similar to salivary SDA. Moreover, TCCRP also harbors recurrent *IDH2* R172X mutations identical to those reported here in SDA.[45–48] Some salivary gland and breast tumor types, including secretory carcinoma and adenoid cystic carcinoma, are regarded as the same entity in both organs due to identical histologic and molecular features across sites. However, other tumors that involve these 2 organs, such as salivary gland epithelial-myoepithelial carcinoma and breast adenomyoepithelioma, are considered separate but analogous entities due to overlapping but not identical clinicopathological and molecular profiles.[30,49–51] The similarities described here suggest that salivary gland SDA and breast TCCRP are another nonidentical analog between these organs.

Finally, these findings demonstrate that IDH1/2 mutation-specific immunohistochemistry is a useful, although imperfect, tool for the diagnosis of SDA. Several commercially-available antibodies recognizing IDH2 R172 mutant protein, usually in combination with its paralog IDH1 R132, have previously been reported as highly sensitive and specific for a wide range of tumors with known *IDH2* mutation, including breast TCCRP.[52–55] And indeed, globular cytoplasmic positivity for IDH1/2 mutant protein was seen in all 9 striated duct neoplasms that were successfully tested, including cases with molecularly-confirmed *IDH2* R172S, R172G, and R172T mutations. Notably, the weak staining with *IDH2* R172T mutation seen here has been reported previously in other tumor types.[54] Interpretation was also complicated by sensitivity to fixation artifact that led to patchy reactivity in 1 case as well as frequent weak cytoplasmic blush in structures or

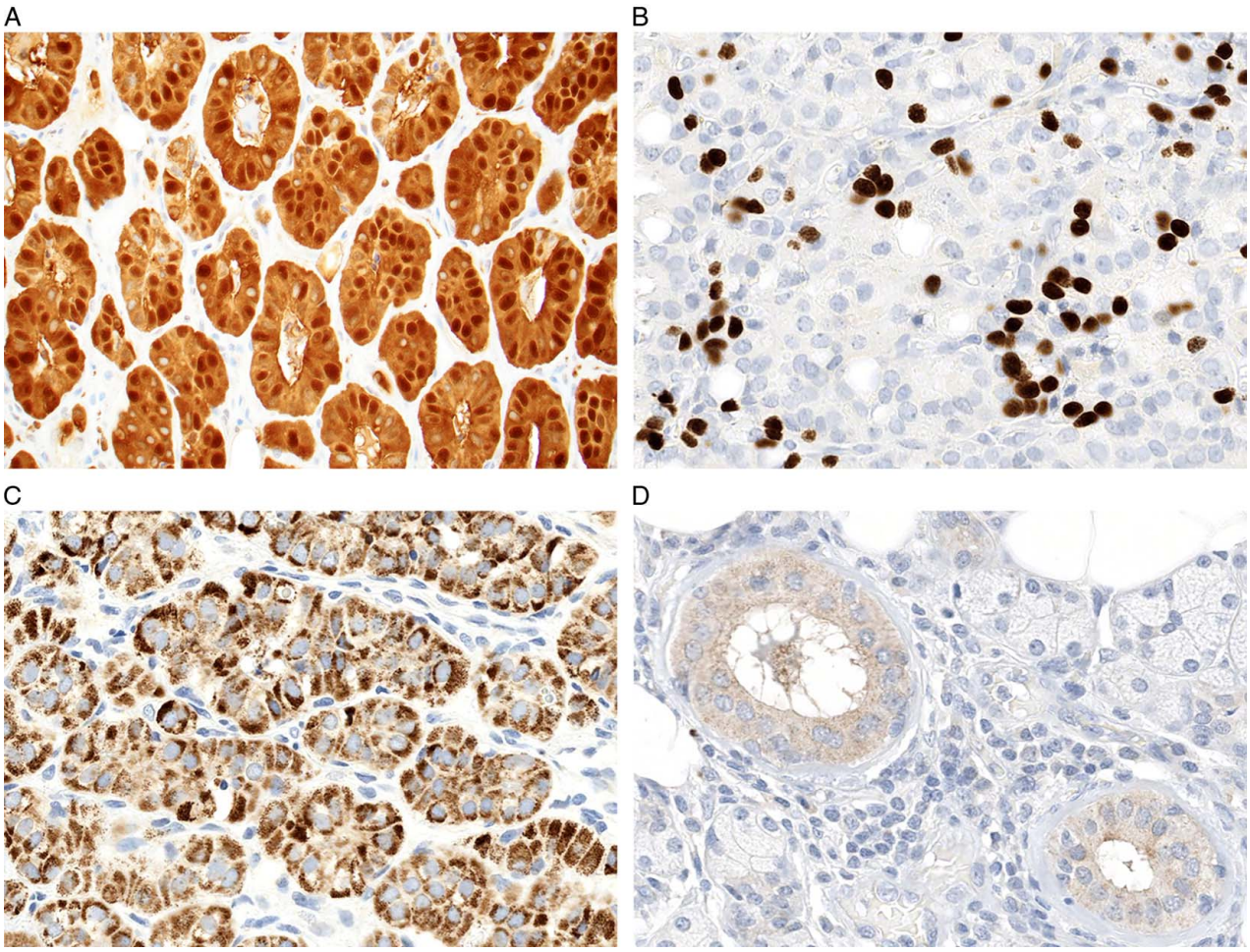

FIGURE 5. Most SDA showed diffuse, strong positivity for S100 protein (A, ×20). A subset of cases showed patchy positivity for p63 in a basal distribution despite no clear histologic evidence of a second cell population (B, ×40). The SDA had diffuse granular to globular positivity for IDH1/2 mutant immunohistochemistry (C, ×40) at a level stronger than the nonspecific blush seen in background striated ducts (D, ×40).

tumors with granular cytoplasm, including normal striated ducts. Notably, although previous studies reported almost perfect specificity for IDH1/2 immunohistochemistry,[53,54] we identified patchy strong reactivity in 4% of salivary tumors assessed on tissue microarray sections, including diffuse staining in 2 salivary duct carcinomas that lacked molecular evidence of *IDH2* or *IDH1* mutations on commercial panels and 2 mucoepidermoid carcinomas with known *MAML2* rearrangement. These findings suggest that, despite some limitations to IDH1/2 mutation-specific immunohistochemistry, diffuse strong staining at levels above background reactivity in normal striated ducts may provide a convenient adjunct for confirming the diagnosis of SDA in the appropriate histologic context.

In summary, despite the rarity of salivary SDA, these tumors display a characteristic histologic and immunohistochemical spectrum that should make them recognizable to pathologists. While the existence of striated duct adenocarcinoma cannot be excluded in tumors that grow adjacent to nerve given the limited sample size and follow-up information, an irregular interface with surrounding salivary tissue should not be interpreted as histologic evidence of malignancy when striated duct features are identified. The presence of recurrent *IDH2* R172X mutations is a defining feature of SDA that allows for the use of IDH1/2 mutation-specific immunohistochemistry to facilitate diagnosis and sets them apart from overlapping lesions such as canalicular adenoma, which has no currently-identifiable genetic alterations. Furthermore, the overall histologic and molecular profile of SDA suggests that they may represent a benign salivary gland analog to breast TCCRP, a recently-described entity that has similar cytology and *IDH2* mutations. Collection of larger numbers of SDA with more extensive follow-up information should allow for a better understanding of their clinicopathologic characteristics in the future.

TABLE 2. IDH1/2 Mutation-Specific Immunohistochemistry in Other Salivary Gland Tumors

Tumor	Positive/n (%)
Acinic cell carcinoma	1/62 (2)
Adenoid cystic carcinoma	3/101 (3)
Basal cell adenoma	0/23 (0)
Basal cell adenocarcinoma	0/4 (0)
Carcinoma NOS	0/47 (0)
Clear cell carcinoma	0/3 (0)
Epithelial-myoepithelial carcinoma	0/24 (0)
Intraductal carcinoma	0/1 (0)
Lymphadenoma	0/6 (0)
Lymphoepithelial carcinoma	0/5 (0)
Mucoepidermoid carcinoma	7/86 (8)
Mucinous adenocarcinoma	0/4 (0)
Myoepithelioma	1/27 (4)
Myoepithelial carcinoma	0/21 (0)
Pleomorphic adenoma	4/22 (18)
Polymorphous adenocarcinoma	0/21 (0)
Salivary duct carcinoma	7/79 (9)
Secretory carcinoma	0/4 (0)
Warthin tumor	0/1 (0)
Total	23/541 (4)

REFERENCES

1. Brazão-Silva MT, Pulino BFB, Pavanello KC, et al. A salivary gland tumor composed by cells with striated duct phenotype: a 'striated duct adenoma'? *Oral Surg Oral Med Oral Pathol Oral Radiol*. 2012;114:E62.
2. Chandwani S, Shah A, Mittal N, et al. Striated duct adenoma of the parotid: A potential diagnostic pitfall. *Indian J Pathol Microbiol*. 2022;65:198–199.
3. Dardick I. Canalicular and Ductal Adenomas. *Color Atlas/Text of Salivary Gland Tumor Pathology*. New York: Igaku-Shoin Medical Publishers, Inc.; 1996:61–66.
4. Ito Y, Fujii K, Murase T, et al. Striated duct adenoma presenting with intra-tumoral hematoma and papillary thyroid carcinoma-like histology. *Pathol Int*. 2017;67:316–321.
5. Mesbah Ardakani N, Parry J, Sterrett G. A case of salivary gland adenoma with ductal differentiation with morphological resemblance to normal striated ducts. *Pathology*. 2015;47:S112.
6. Weinreb I, Simpson RH, Skalova A, et al. Ductal adenomas of salivary gland showing features of striated duct differentiation ('striated duct adenoma'): a report of six cases. *Histopathology*. 2010;57:707–715.
7. Bloemena E, Katabi N. Canalicular adenoma and other ductal adenomas. In: El-Naggar A, Chan JK, Grandis JR, et al, eds. *WHO Classification of Head and Neck Tumours*. Lyon, France: International Agency for Research on Cancer; 2017:194.
8. Weinreb I, Hellquist H, Perez-Ordonez B, et al. Striated duct adenoma. In: WHO Classification of Tumours Editorial. In: Board, ed. *WHO Classification of Head and Neck Tumours*. Lyon, France: International Agency for Research on Cancer; 2022.
9. Rooper LM, Mansour M, Yonescu R, et al. The decline of salivary adenocarcinoma not otherwise specified as a tumor entity: Reclassification using contemporary immunohistochemical profiling and diagnostic criteria. *Am J Surg Pathol*. 2021;45:753–764.
10. Bishop JA, Gagan J, Baumhoer D, et al. Sclerosing polycystic "adenosis" of salivary glands: a neoplasm characterized by PI3K pathway alterations more correctly named sclerosing polycystic adenoma. *Head Neck Pathol*. 2020;14:630–636.
11. Bishop JA, Yonescu R, Batista D, et al. Mucoepidermoid carcinoma does not harbor transcriptionally active high risk human papillomavirus even in the absence of the MAML2 translocation. *Head Neck Pathol*. 2014;8:298–302.
12. Rettig EM, Talbot CC Jr, Sausen M, et al. Whole-genome sequencing of salivary gland adenoid cystic carcinoma. *Cancer Prev Res (Phila)*. 2016;9:265–274.
13. Andreasen S, Varma S, Barasch N, et al. The HTN3-MSANTD3 fusion gene defines a subset of acinic cell carcinoma of the salivary gland. *Am J Surg Pathol*. 2019;43:489–496.
14. Rooper LM, Lombardo KA, Oliai BR, et al. MYB RNA In situ hybridization facilitates sensitive and specific diagnosis of adenoid cystic carcinoma regardless of translocation status. *Am J Surg Pathol*. 2021;45:488–497.
15. McHugh JB, Hoschar AP, Dvorakova M, et al. p63 immunohistochemistry differentiates salivary gland oncocytoma and oncocytic carcinoma from metastatic renal cell carcinoma. *Head Neck Pathol*. 2007;1:123–131.
16. Magliocca KR, Seethala RR. Salivary intercalated duct lesions in transition. *Histopathology*. 2016;69:710–711.
17. Losman JA, Kaelin WG Jr. What a difference a hydroxyl makes: mutant IDH, (R)-2-hydroxyglutarate, and cancer. *Genes Dev*. 2013;27:836–852.
18. Tommasini-Ghelfi S, Murnan K, Kouri FM, et al. Cancer-associated mutation and beyond: The emerging biology of isocitrate dehydrogenases in human disease. *Sci Adv*. 2019;5:eaaw4543.
19. Yang H, Ye D, Guan KL, et al. IDH1 and IDH2 mutations in tumorigenesis: mechanistic insights and clinical perspectives. *Clin Cancer Res*. 2012;18:5562–5571.
20. Amary MF, Bacsi K, Maggiani F, et al. IDH1 and IDH2 mutations are frequent events in central chondrosarcoma and central and periosteal chondromas but not in other mesenchymal tumours. *J Pathol*. 2011;224:334–343.
21. Borger DR, Tanabe KK, Fan KC, et al. Frequent mutation of isocitrate dehydrogenase (IDH)1 and IDH2 in cholangiocarcinoma identified through broad-based tumor genotyping. *Oncologist*. 2012;17:72–79.
22. Marcucci G, Maharry K, Wu YZ, et al. IDH1 and IDH2 gene mutations identify novel molecular subsets within de novo cytogenetically normal acute myeloid leukemia: a Cancer and Leukemia Group B study. *J Clin Oncol*. 2010;28:2348–2355.
23. Yan H, Parsons DW, Jin G, et al. IDH1 and IDH2 mutations in gliomas. *N Engl J Med*. 2009;360:765–773.
24. Dogan S, Chute DJ, Xu B, et al. Frequent IDH2 R172 mutations in undifferentiated and poorly-differentiated sinonasal carcinomas. *J Pathol*. 2017;242:400–408.
25. Jo VY, Chau NG, Hornick JL, et al. Recurrent IDH2 R172X mutations in sinonasal undifferentiated carcinoma. *Mod Pathol*. 2017;30:650–659.
26. Chiosea SI, Williams L, Griffith CC, et al. Molecular characterization of apocrine salivary duct carcinoma. *Am J Surg Pathol*. 2015;39:744–752.
27. Dalin MG, Desrichard A, Katabi N, et al. Comprehensive molecular characterization of salivary duct carcinoma reveals actionable targets and similarity to apocrine breast cancer. *Clin Cancer Res*. 2016;22:4623–4633.
28. Dalin MG, Katabi N, Persson M, et al. Multi-dimensional genomic analysis of myoepithelial carcinoma identifies prevalent oncogenic gene fusions. *Nat Commun*. 2017;8:1197.
29. Dogan S, Ng CKY, Xu B, et al. The repertoire of genetic alterations in salivary duct carcinoma including a novel HNRNPH3-ALK rearrangement. *Hum Pathol*. 2019;88:66–77.
30. El Hallani S, Udager AM, Bell D, et al. Epithelial-myoepithelial carcinoma: frequent morphologic and molecular evidence of preexisting pleomorphic adenoma, common HRAS mutations in PLAG1-intact and HMGA2-intact Cases, and occasional TP53, FBXW7, and SMARCB1 alterations in high-grade cases. *Am J Surg Pathol*. 2018;42:18–27.
31. Gargano SM, Senarathne W, Feldman R, et al. Novel therapeutic targets in salivary duct carcinoma uncovered by comprehensive molecular profiling. *Cancer Med*. 2019;8:7322–7329.
32. Grunewald I, Vollbrecht C, Meinrath J, et al. Targeted next generation sequencing of parotid gland cancer uncovers genetic heterogeneity. *Oncotarget*. 2015;6:18224–18237.
33. Ho AS, Kannan K, Roy DM, et al. The mutational landscape of adenoid cystic carcinoma. *Nat Genet*. 2013;45:791–798.
34. Kang H, Tan M, Bishop JA, et al. Whole-exome sequencing of salivary gland mucoepidermoid carcinoma. *Clin Cancer Res*. 2017;23:283–288.

35. Karpinets TV, Mitani Y, Liu B, et al. Whole-genome sequencing of common salivary gland carcinomas: subtype-restricted and shared genetic alterations. *Clin Cancer Res*. 2021;27:3960–3969.
36. Mueller SA, Gauthier MA, Blackburn J, et al. Molecular patterns in salivary duct carcinoma identify prognostic subgroups. *Mod Pathol*. 2020;33:1896–1909.
37. Rack S, Feeney L, Hapuarachi B, et al. Evaluation of the Clinical Utility of Genomic Profiling to Inform Selection of Clinical Trial Therapy in Salivary Gland Cancer. *Cancers*. 2022;14.
38. Ross JS, Gay LM, Wang K, et al. Comprehensive genomic profiles of metastatic and relapsed salivary gland carcinomas are associated with tumor type and reveal new routes to targeted therapies. *Ann Oncol*. 2017;28:2539–2546.
39. Stephens PJ, Davies HR, Mitani Y, et al. Whole exome sequencing of adenoid cystic carcinoma. *J Clin Invest*. 2013;123:2965–2968.
40. Wang K, McDermott JD, Schrock AB, et al. Comprehensive genomic profiling of salivary mucoepidermoid carcinomas reveals frequent BAP1, PIK3CA, and other actionable genomic alterations. *Ann Oncol*. 2017;28:748–753.
41. Wang K, Russell JS, McDermott JD, et al. Profiling of 149 salivary duct carcinomas, carcinoma ex pleomorphic adenomas, and adenocarcinomas, not otherwise specified reveals actionable genomic alterations. *Clin Cancer Res*. 2016;22:6061–6068.
42. Thompson LD, Bauer JL, Chiosea S, et al. Canalicular adenoma: a clinicopathologic and immunohistochemical analysis of 67 cases with a review of the literature. *Head Neck Pathol*. 2015;9:181–195.
43. Agaimy A, Ihrler S, Baneckova M, et al. HMGA2-WIF1 rearrangements characterize a distinctive subset of salivary pleomorphic adenomas with prominent trabecular (canalicular adenoma-like) morphology. *Am J Surg Pathol*. 2022;46:190–199.
44. Yang WT, Bu H, Foschini MP, et al. WHO Classification of Tumours Editorial Board. Tall cell carcinoma with reversed polarity. *WHO Classification of Breast Tumours*. Lyon, France: International Agency for Research on Cancer; 2021.
45. Bhargava R, Florea AV, Pelmus M, et al. Breast tumor resembling tall cell variant of papillary thyroid carcinoma: a solid papillary neoplasm with characteristic immunohistochemical profile and few recurrent mutations. *Am J Clin Pathol*. 2017;147:399–410.
46. Chiang S, Weigelt B, Wen HC, et al. IDH2 mutations define a unique subtype of breast cancer with altered nuclear polarity. *Cancer Res*. 2016;76:7118–7129.
47. Lozada JR, Basili T, Pareja F, et al. Solid papillary breast carcinomas resembling the tall cell variant of papillary thyroid neoplasms (solid papillary carcinomas with reverse polarity) harbour recurrent mutations affecting IDH2 and PIK3CA: a validation cohort. *Histopathology*. 2018;73:339–344.
48. Zhong E, Scognamiglio T, D'Alfonso T, et al. Breast tumor resembling the tall cell variant of papillary thyroid carcinoma: molecular characterization by next-generation sequencing and histopathological comparison with tall cell papillary carcinoma of thyroid. *Int J Surg Pathol*. 2019;27:134–141.
49. Geyer FC, Li A, Papanastasiou AD, et al. Recurrent hotspot mutations in HRAS Q61 and PI3K-AKT pathway genes as drivers of breast adenomyoepitheliomas. *Nat Commun*. 2018;9:1816.
50. Ginter PS, McIntire PJ, Kurtis B, et al. Adenomyoepithelial tumors of the breast: molecular underpinnings of a rare entity. *Mod Pathol*. 2020;33:1764–1772.
51. Lubin D, Toorens E, Zhang PJ, et al. Adenomyoepitheliomas of the breast frequently harbor recurrent hotspot mutations in PIK3-AKT pathway-related genes and a subset show genetic similarity to salivary gland epithelial-myoepithelial carcinoma. *Am J Surg Pathol*. 2019;43:1005–1013.
52. Alsadoun N, MacGrogan G, Truntzer C, et al. Solid papillary carcinoma with reverse polarity of the breast harbors specific morphologic, immunohistochemical and molecular profile in comparison with other benign or malignant papillary lesions of the breast: a comparative study of 9 additional cases. *Mod Pathol*. 2018;31:1367–1380.
53. Dogan S, Frosina D, Geronimo JA, et al. Molecular epidemiology of IDH2 hotspot mutations in cancer and immunohistochemical detection of R172K, R172G, and R172M variants. *Hum Pathol*. 2020;106:45–53.
54. Mito JK, Bishop JA, Sadow PM, et al. Immunohistochemical detection and molecular characterization of IDH-mutant sinonasal undifferentiated carcinomas. *Am J Surg Pathol*. 2018;42:1067–1075.
55. Pareja F, da Silva EM, Frosina D, et al. Immunohistochemical analysis of IDH2 R172 hotspot mutations in breast papillary neoplasms: applications in the diagnosis of tall cell carcinoma with reverse polarity. *Mod Pathol*. 2020;33:1056–1064.